Supporting information

A. Fire prediction methods – a review

As shown in Table S1, there are three main approaches for the prediction of wildfire. Among them, regression is the most widely used, with the goal of deriving a relationship between fire parameters (e.g., area burned or probability) and meteorological, hydrological, and geographic variables. Different forms of regression have been adopted, such as stepwise (Flannigan et al., 2005; McCoy and Burn, 2005; Amiro et al., 2009; Spracklen et al., 2009), exponential (Drever et al., 2009), and logistic regression (Krawchuk et al., 2009b; Westerling et al., 2011) as well as Multivariate Adaptive Regression Spline (MARS) (Balshi et al., 2009). The regression approach usually has a reasonable predictive capability, with R^2 ranging from 0.3 to 0.8. It is numerically efficient because it usually employs monthly or seasonal variables averaged over a large spatial scale (e.g., Flannigan et al., 2005; Littell et al., 2009). Obtaining satisfactory fits (or correlations) usually requires aggregating area burned data into large ecoregions (e.g., Flannigan et al., 2005; Amiro et al., 2009; Spracklen et al., 2009), smoothing the meteorological data (e.g., Littell et al., 2009; Rasilla et al., 2010), or adopting a series of complex multiplicative relationships (e.g., Drever et al., 2009; Westerling et al., 2011).

The regression methods also have significant limitations. For the stepwise regression method, which selects predictors based on their correlations with the predictand, the more potential predictors used, the more robust the fit. However, an increase in the number of terms may also result in some terms closely correlating with each other. Such collinearity not only makes it difficult to isolate contributions from individual factors (Moritz et al., 2012), but also may result in mathematical instability in future projections (Philippi, 1993). Another limitation is that a change in the length of the time series or use of a different meteorological dataset may lead to a different order of terms in the regression fit (e.g. Littell et al., 2009), causing very different projections using meteorological output from a GCM. Other regression methods, such as MARS or a probabilistic approach, may avoid collinearity among predictors, but have their own limitations. For example, the MARS technique can develop good regression fits on small spatial scales, but interpretation of these fits may be challenging due to the complicated functional forms

for the predictor variables and the large number of functions. The probabilistic method has good potential for predicting fire frequency; however, transforming the calculated frequency to area burned requires making many assumptions (Westerling et al., 2011).

Parameterizations or process-based fire models adopt uniform functions for all grid cells in a model or region (e.g. Cardoso et al., 2003; Arora and Boer, 2005; Crevoisier et al., 2007; Pechony and Shindell, 2009). The parameterization usually employs nonlinear relations between fire and environmental variables, in contrast to regression methods that often assume linear responses. However, most previous parameterizations have proven difficult to evaluate, especially on a global scale, in part due to a paucity of observations. For example, Kloster et al. (2010) used two satellite products to evaluate simulations of area burned, but noted that there are large discrepancies between the two products, making validation difficult on a global scale. In addition, the prediction of area burned is especially challenging for parameterizations. Some models capture reasonable patterns of fire probability or fire occurrence, but show large biases for area burned (e.g., Crevoisier et al., 2007). Also, the constants in some of the parameterization functions are determined a posteriori based on empirical or statistical fits, which limits their application to regions where observed fire data are available (e.g., Crevoisier et al., 2007).

Both the regression method and the parameterizations neglect the effects of wildfires on the biosphere, as well as the impact of climate change on vegetation type and extent. DGVMs may address these shortcomings by dynamically simulating fire activity (e.g., Kloster et al., 2010; Thonicke et al., 2010). DGVM projections of fire activity allow for the feedbacks among climate, biosphere and fires and can be used to quantify the contributions of different factors to trends in fire activity (Kloster et al., 2012). However, the fire schemes implemented in DGVMs are relatively simple compared to other elements of these models (Krawchuk et al., 2009a). In addition, vegetation type simulated in DGVMs show large inter-model variability on both regional and global scales (Bachelet et al., 2003; Purves and Pacala, 2008), and the simulated fire patterns can show large biases over North America (Kelley et al., 2012). DGVMs are computationally expensive, so that driving a DGVM with output from an array of GCMs would be a large undertaking.

Clearly, different approaches have their strengths and weaknesses. We choose to apply both a regression and a parameterization method to depict the response of area burned to the changing climate. These two approaches have contrasting advantages, and their application helps to quantify the uncertainties in the fire projections. Use of a DGVM is not practical for this work since our goal is to develop efficient methods to quantify both the magnitude and uncertainty of fire activity in 15 climate models.

B. Canadian Fire Weather Index system

The Canadian Fire Weather Index system (CFWIS, Van Wagner, 1987) calculates seven fire indexes that characterize the impact of temperature, fuel moisture, and wind speed on fire behavior (http://cwfis.cfs.nrcan.gc.ca/background/summary/fwi). The Fine Fuel Moisture Code (FFMC), Duff Moisture Code (DMC), and Drought Code (DC) indicate moisture levels for litter fuels, loosely compacted organic layers of moderate depth, and deep organic layers. The Initial Spread Index (ISI), Build-up Index (BUI), and Fire Weather Index (FWI) represent the rate of fire spread, fuel availability, and fire intensity. These indexes are calculated from the three fuel moisture codes and their values rise as the fire danger increases. The Daily Severity Rating (DSR) is an exponential function of the FWI, indicating the difficulty in controlling fires. These fire indexes were used as potential predictors in previous regression studies (e.g. Flannigan et al., 2005; Amiro et al., 2009). There are other fire index systems, such as U.S. National Forest Fire Danger Rating System, which also provide quantification of fire-weather relationships. However, these systems require hourly meteorological data as input (National Wildfire Coordinating Group, 2005), which are not available in either the site-based observations or the climate model output used in this study.

To calculate CFWIS indexes, we use daily data from the Global Surface Summary of the Day (GSOD, http://www.ncdc.noaa.gov/cgi-bin/res40.pl?page=gsod.html), which provides 18 daily surface meteorological elements for over 1600 stations in the western U.S. We select a given station if at least two-thirds of its records are available between 1978 and 2004, resulting in 234 sites distributed fairly evenly over western U.S. We use the daily mean and maximum temperature, dew point temperature, precipitation, and mean wind speed, and we calculate daily mean relative humidity (*RH*) from the daily

mean temperature and dew point temperature. The above variables are binned into ecoregions after the elevation correction described in Spracklen et al. (2009).

C. Additional evaluations of regressions

To quantify the stability of our regressions, we apply "leave-one-out" cross-validation, which estimates regression coefficients based on all the data except for one point and makes a prediction for that point each round. The R^2 from the cross-validation remains as high as 0.46-0.49 in two forest ecoregions but shows a low value of 0.13 in California Coastal Shrub. Observations show that extreme events dominate the total area burned over a period of several years (Fig. 3). Fire models, however, tend to have difficulty capturing these extreme events (Bachelet et al., 2005; Crevoisier et al., 2007; Balshi et al., 2009; Spracklen et al., 2009; Westerling et al., 2011), possibly because they omit some nonlinear responses. For example, Westerling et al. (2011) underestimated area burned for the 1988 Yellowstone fire by 60%, even though they obtained a very good estimate (R^2= 0.83) of fire occurrence in a given year based on several assumptions in their regressions. To test the model representation of extreme fire events, we examine the model predictions for the top three large fire years in each ecoregion. The regressions underestimate area burned by 20-60% for these extreme years. In the two forest ecoregions, area burned during extreme years is underestimated by 20-40%.

D. Additional evaluations of the parameterization

Fig. S1 compares the modeled spatial pattern of the annual mean area burned to observations. The parameterization reproduces the large values in the Pacific Northwest, Nevada Mountains /Semi-desert, and California Coastal Shrub ecoregions, but underestimates area burned by 80% in central Idaho, a region with abundant fuel loads. The area burned in grasslands, such as eastern Colorado, Wyoming, and eastern Montana, is overestimated by 70%. The spatial correlation coefficient between the parameterization and observation is low, 0.33 for 331 grid points, because of these deficiencies.

Fig. S2 compares the simulated seasonality of area burned with observations in each ecoregion. The prediction reproduces the seasonality in the Desert Southwest, Nevada Mountains/Semi-desert, Rocky Mountains Forest, and Eastern Rocky Mountains/Great

Plains, mainly because area burned in these regions follows the seasonality of temperature, relative humidity, and precipitation. The parameterization overestimates the area burned in September in the Pacific Northwest but fails to capture the October peak in the California Costal Shrub region, where the Santa Ana winds enhance wildfire activity (Schroeder et al., 1964).

E. Evaluations of present-day prediction with GCM meteorology

For the regressions, the median GCM-driven result matches the observed area burned within ±11%, except for the Rocky Mountains Forest where area burned is overestimated by 45% (Table 3). For the western United States, area burned is overestimated by 16%. There is a relatively small spread in the ratio of predicted to observed area burned for the GCM results for Desert Southwest and Nevada Mountains /Semi-desert, but a large spread for the Rocky Mountains Forest (Fig. S3a). Since the mean meteorological fields from the GCMs have been scaled with mean observations, the spread in the predictions is larger in ecoregions for which the leading term in the regression is one of the fire weather indexes (Table 1).

For the parameterization, there is also good agreement with observed area burned for median GCM results, with the largest discrepancy in Eastern Rocky Mountains/Great Plains, where this method underestimates area burned by 24% (Table 4). The spread of the predictions with the parameterization (Fig. S3b) is generally larger than that with the regression method because of the exponential relationship between area burned and meteorological variables. The predictions exhibit a large spread in the Pacific Northwest and Rocky Mountains Forest, with two models as outliers (Fig. S3b). These models predict extreme weather conditions (e.g., very low relative humidity and/or high temperature) for some days, leading to very high values for area burned.

F. Ensemble projection of future climate change

Fig. S4 shows projected median changes in key meteorological fields, calculated from the 15 climate models under the A1B scenario. Median temperatures over the western United States increase by 2.0°C in winter and by 2.4°C in summer by midcentury, relative to the present day. In winter, precipitation increases by 0.2 mm day^{-1} at latitudes

poleward of 40°N, and by 0.4 mm day^{-1} in the Pacific Northwest. This result is consistent with the projected weakening of the meridional temperature gradient, which leads to a poleward shift of mid-latitude storm tracks and precipitation (Yin, 2005). In particular, an intensified Aleutian Low in the 2050s atmosphere strengthens storm tracks in winter and increases moisture transport to mid-to-high latitudes (Salathe, 2006). A decline in precipitation in western U.S. in JJA and the southern U.S. in DJF is consistent with a poleward expansion of the subtropical subsiding branch of the Hadley circulation in the future atmosphere (Hu et al., 2007; Lu et al., 2007). In summer, the GCMs project a median decrease of 0.06 mm day^{-1} in precipitation (Fig. S4d). Specific humidity increases by 0.3 g kg^{-1} in winter and 0.8 g kg^{-1} in summer, at least in part because of the higher temperatures. However, the annual mean relative humidity decreases by 1% over the western United States.

The predicted changes in summer mean temperature, precipitation, and relative humidity for the climate models are shown in Fig. S5. In all ecoregions, median temperatures increase at least by 2 °C. Although there is a large spread among models, the change in temperature is significant ($p < 0.05$). The median values of precipitation decrease by ~0.1 mm day^{-1} in the Pacific Northwest, Nevada Mountains/ Semi-desert, and Rocky Mountains Forest, but show little change elsewhere. Median relative humidity decreases by 0.6-0.8% over the western U.S., except in California Coastal Shrub ecoregion where the median increases by 0.4%.

G. Estimate of future fuel consumption

We explored whether changes in vegetation would affect fuel consumption on a time scale of 50 years using the Lund-Potsdam-Jena (LPJ) DGVM (Prentice et al., 2000; Sitch et al., 2003). This model simulates the changes in vegetation type in response to changes in climate and CO_2 on a global scale. Monthly meteorological anomalies, including temperature, precipitation, and cloud fraction from the GISS GCM3 were used to drive the LPJ model at resolution of 1°×1° for 1980-2050 (Wu et al., 2012). The averages during 1990-2000 are used for the present day and those for 2040-2050 for midcentury.

The LPJ DGVM does not simulate fuel consumption, although it calculates the total carbon in plants and soil. The model simulates six different vegetation types over western

U.S. and C3 perennial grass is the most dominant one (Table S2). We build a regression between the six vegetation cover fractions from LPJ DGVM and the fuel consumption from FCCS on the basis of grid boxes. We use the regression coefficient as the consumption value for each kind of plant. As Table S2 shows, two types of needleleaved trees cover only 21% of the land surface but account for over 60% of the total fuel consumption at present day. On the other hand, the carbon consumption from grassland accounts for less than 3% of present-day values.

With the estimated coefficients and the projected changes in cover fraction (Table S2), we found little change (<0.1%) in fuel consumption averaged over the western U.S. by the midcentury. Our results are consistent with those from Zhang et al. (2010), who investigated the response of FCCS fuel load in the southern United States to future climate and found small changes by midcentury. However, meteorological changes and increasing CO_2 levels could together lead to large regional changes in fuel consumption. The LPJ model projects some desert amelioration in southwestern area, consistent with Bachelet et al. (2001). For this project, we assume that fuel consumption throughout the western U.S. remains constant, an approach that likely leads to an underestimate of future fire emissions in populous regions such as the southern California. Calculation of a detailed ecosystem response to the future climate generated by the full array of CMIP3 models is, however, beyond the scope of the current project.

H. Gridded area burned from the projections

The regressions provide the total area burned during the fire season, while the parameterization provides gridded area burned (1º×1º) on a daily scale. As noted in section D of this SI, the predicted spatial pattern does not match that observed very well at the grid box level, and this translates into errors in biomass burned. The parameterization performs better on the scale of ecoregions (Fig. 5), so we sum the 1º×1º grids within each ecosystem, and then disaggregate them as described below for use in the CTM.

We spatially allocate area burned within each ecoregion with a random approach, building on the work in Spracklen et al. (2009). For the regressions, we first convert the median values of the predicted annual area burned (Table 3) to monthly values using the

observed seasonality during 1980-2004 in each ecoregion, assuming that the seasonality does not change from present day to midcentury. For the parameterization, we calculate the monthly total area burned over each ecoregion based on the daily gridded predictions from each GCM, and use these to derive the ensemble medians. Spracklen et al. (2009) showed that for all ecoregions, 70% of area burned occurs in 5-25% of the grid boxes in the ecoregion (Fig. 7 in Spracklen et al. (2009)) and therefore placed 70% of the predicted area burned randomly in 10% of grid cells in each ecoregion.

However, the observed area burned is not randomly distributed over the ecosystems within each ecoregion, as shown in Table S3. We distribute the area burned according to the present-day fractions among the ecosystems, and distribute them randomly within each sub-unit. For California Coastal Shrub and Nevada Mountains /Semi-desert ecoregions where the parameterization has no predictive capability, we simply apply present-day area burned to the calculation of future biomass burned. These ecoregions account for only 14% of the total biomass consumption over the western United States (Table 6). As a result, using constant, present-day emissions there should not greatly affect our predictions. The random method minimizes the possibility of reburning in grid squares. To evaluate the potential error in assuming no reburning, we conduct the same sensitivity test as in Spracklen et al. (2009): we assume no regrowth of vegetation after a fire and reset fuels to zero. Using the future area burned predicted by the parameterization, we calculate 22% less fuel burned in this extreme case than in the case with constant fuel load for 2046-2055 over 50 years.

Table S1 Studies projecting future area burned in North America

Fire model	Region	Scenario and period	# GCMs	Projected changes	Reference
Regression	Canada	$2\times CO_2$ vs. $1\times CO_2$	3	+ 40%	Flannigan and Van Wagner (1991)
Regression	USA	$2\times CO_2$ vs. $1\times CO_2$	1	+ 78%	Price and Rind (1994)
DGVM [a]	USA	1995-2100 vs. 1895-1994	2	+ 4-31%	Bachelet et al. (2003)
Regression	Western Canada	$3\times CO_2$ (2080-2100) vs. $1\times CO_2$ (1975-1990)	1	+ 14-137%	de Groot et al. (2003)
Parameterization	USA (northern California)	$2\times CO_2$ vs. $1\times CO_2$	1	+ 50%	Fried et al. (2004)
DGVM	USA (Alaska)	2050-2100 vs. 1950-2000	2	+ 17-39%	Bachelet et al. (2005)
Regression	Canada	$3\times CO_2$ (2080-2099) vs. $1\times CO_2$ (1959-1997)	2	+ 74-118%	Flannigan et al. (2005)
Regression	Canada (Yukon)	Multiple scenarios at 2040-2069 vs. 1961-1990	8	+ 33% (mean) + 227 (max)	McCoy and Burn (2005)
Parameterization	Canada (Alberta)	$2\times CO_2$ (2040-2049)or $3\times CO_2$ (2080-2089) vs. $1\times CO_2$	1	+ 13% or 29%	Tymstra et al. (2007)
DGVM	USA (California)	2050-2099 vs. 1895-2003	2	+ 9-15%	Lenihan et al. (2008)
Regression	Canada	$2\times CO_2$ or $3\times CO_2$ vs. $1\times CO_2$	1	+ 34% or 93%	Amiro et al. (2009)
Regression	Alaska and west Canada	A2 and B2 scenarios at 2041-2050 vs. 1991-2000	1	+ 100%	Balshi et al. (2009)
Regression	Canada (Quebec)	A1B, A2, B1, and B2 scenarios at 2100 vs. 1959-1999	2	+ 20-700%	Drever et al. (2009)
Regression	Canada (Alberta)	$2\times CO_2$ (2040-2049) or $3\times CO_2$ (2080-2089) vs. $1\times CO_2$	1	+ 90% or 160%	Krawchuk et al. (2009b)
Regression	Western USA	A1B scenario at 2046-2055 vs. 1996-2005	1	+ 54%	Spracklen et al. (2009)
DGVM	USA (Pacific Northwest)	A2 scenario at 2070-2099 vs. 1971-2000	3	+ 76-310%	Rogers et al. (2011)
Regression	USA (Yellowstone)	A2 scenario At 2035-2064 vs. 1961-1990	3	+ 230-900%	Westerling et al. (2011)

[a] DGVM: Dynamic Global Vegetation Model

Table S2 Simulated changes in the vegetation cover fraction by LPJ DGVM

Vegetation types in LPJ DGVM	Estimated Fuel Consumption [a] (Kg DM m^{-2})	Cover fraction (%)	
		2000	2050
Temperate needleleaved evergreen tree	6.46	6.7	7.7
Temperate broadleaved evergreen tree	2.98	2.7	3.3
Temperate broadleaved summergreen tree	1.84	17.5	22.9
Boreal needleleaved evergreen tree	3.75	14.4	10.6
Boreal summergreen tree	2.3	8.0	6.2
C3 perennial grass	0.1	38.3	41.0

[a] Estimated as the coefficients c_n in regression $\sum_{n=1}^{6} c_n F_{n,i} = T_i$, where $F_{n,i}$ is the cover fraction for vegetation type n on grid i and T_i is the FCCS fuel consumption (including live and dead fuels) on the same grid.

Table S3 Area and area burned fraction of each Bailey ecosystem [a] to the corresponding aggregated ecoregion [b] during 1980-2004.

Ecoregions	Area Frac (%)	Area burned Frac (%)	Ecoregions	Area Frac (%)	Area burned Frac (%)
Pacific Northwest			Nevada /Semi-desert		
242	8	0	341	38	36
m242	42	33	m341	14	10
m261	50	67	342	48	54
Cal. Coastal Shrub			Rocky Mnts Forest		
262	29	16	m331	46	24
m262	41	68	m332	36	59
261	30	16	m333	18	17
Desert Southwest			Great Plains		
322	31	34	331	79	98
321	21	20	315	21	2
m313	19	24			
313	29	22			

[a] Refer to http://www.fs.fed.us/rm/ecoregions/products/ for the spatial distribution of each Bailey ecosystem in western United States.

[b] Refer to Fig. 2 in Spracklen et al. (2009) for the relations between Bailey ecosystems and the aggregated ecoregions.

References

Amiro, B. D., Cantin, A., Flannigan, M. D., and de Groot, W. J., 2009. Future emissions from Canadian boreal forest fires. Canadian Journal of Forest Research 39, 383-395, doi:10.1139/X08-154.

Arora, V. K., and Boer, G. J., 2005. Fire as an interactive component of dynamic vegetation models. J. Geophys. Res. 110, G02008, doi:10.1029/2005jg000042.

Bachelet, D., Neilson, R. P., Lenihan, J. M., and Drapek, R. J., 2001. Climate change effects on vegetation distribution and carbon budget in the United States. Ecosystems 4, 164-185.

Bachelet, D., Neilson, R. P., Hickler, T., Drapek, R. J., Lenihan, J. M., Sykes, M. T., Smith, B., Sitch, S., and Thonicke, K., 2003. Simulating past and future dynamics of natural ecosystems in the United States. Global Biogeochemical Cycles 17, doi:10.1029/2001gb001508.

Bachelet, D., Lenihan, J., Neilson, R., Drapek, R., and Kittel, T., 2005. Simulating the response of natural ecosystems and their fire regimes to climatic variability in Alaska. Canadian Journal of Forest Research 35, 2244-2257, doi:10.1139/X05-086.

Balshi, M. S., McGuirez, A. D., Duffy, P., Flannigan, M., Walsh, J., and Melillo, J., 2009. Assessing the response of area burned to changing climate in western boreal North America using a Multivariate Adaptive Regression Splines (MARS) approach. Global Change Biology 15, 578-600, doi:10.1111/J.1365-2486.2008.01679.X.

Cardoso, M. F., Hurtt, G. C., Moore, B., Nobre, C. A., and Prins, E. M., 2003. Projecting future fire activity in Amazonia. Global Change Biology 9, 656-669, doi:10.1046/j.1365-2486.2003.00607.x.

Crevoisier, C., Shevliakova, E., Gloor, M., Wirth, C., and Pacala, S., 2007. Drivers of fire in the boreal forests: Data constrained design of a prognostic model of burned area for use in dynamic global vegetation models. Journal of Geophysical Research 112, D24112, doi:10.1029/2006jd008372.

de Groot, W. J., Bothwell, P. M., Carlsson, D. H., and Logan, K. A., 2003. Simulating the effects of future fire regimes on western Canadian boreal forests. Journal of Vegetation Science 14, 355-364.

Drever, C. R., Bergeron, Y., Drever, M. C., Flannigan, M., Logan, T., and Messier, C., 2009. Effects of climate on occurrence and size of large fires in a northern hardwood landscape: historical trends, forecasts, and implications for climate change in Temiscamingue, Quebec. Applied Vegetation Science 12, 261-272.

Flannigan, M. D., and Van Wagner, C. E., 1991. Climate Change and Wildfire in Canada. Canadian Journal of Forest Research 21, 66-72.

Flannigan, M. D., Logan, K. A., Amiro, B. D., Skinner, W. R., and Stocks, B. J., 2005. Future area burned in Canada. Climatic Change 72, 1-16, doi:10.1007/S10584-005-5935-Y.

Fried, J. S., Torn, M. S., and Mills, E., 2004. The impact of climate change on wildfire severity: A regional forecast for northern California. Climatic Change 64, 169-191.

Hu, Y., and Fu, Q., 2007. Observed poleward expansion of the Hadley circulation since 1979. Atmospheric Chemistry and Physics 7, 5229-5236.

Lu, J., Vecchi, G. A., and Reichler, T., 2007. Expansion of the Hadley cell under global warming. Geophysical Research Letter 34, doi:10.1029/2006GL028443.

Kelley, D. I., Prentice, I. C., Harrison, S. P., Wang, H., Simard, M., Fisher, J. B., and Willis, K. O., 2012. A comprehensive benchmarking system for evaluating global vegetation models. Biogeosciences Discuss 9, 15723-15785, doi:10.5194/bgd-9-15723-2012.

Kloster, S., Mahowald, N. M., Randerson, J. T., Thornton, P. E., Hoffman, F. M., Levis, S., Lawrence, P. J., Feddema, J. J., Oleson, K. W., and Lawrence, D. M., 2010. Fire dynamics during the 20th century simulated by the Community Land Model. Biogeosciences 7, 1877-1902, doi:10.5194/bgd-7-565-2010.

Kloster, S., Mahowald, N. M., Randerson, J. T., and Lawrence, P. J., 2012. The impacts of climate, land use, and demography on fires during the 21st century simulated by CLM-CN. Biogeosciences 9, 509-525, doi:10.5194/Bg-9-509-2012.

Krawchuk, M. A., Moritz, M. A., Parisien, M. A., Van Dorn, J., and Hayhoe, K., 2009a. Global pyrogeography: macro-scaled statistical models for understanding the current and future distribution of fire. Plos One 4, e5102, doi:10.1371/journal.pone.0005102.

Krawchuk, M. A., Cumming, S. G., and Flannigan, M. D., 2009b. Predicted changes in fire weather suggest increases in lightning fire initiation and future area burned in the

mixedwood boreal forest. Climatic Change 92, 83-97, doi:10.1007/S10584-008-9460-7.

Lenihan, J. M., Bachelet, D., Neilson, R. P., and Drapek, R., 2008. Response of vegetation distribution, ecosystem productivity, and fire to climate change scenarios for California. Climatic Change 87, S215-S230, doi:10.1007/S10584-007-9362-0.

Littell, J. S., McKenzie, D., Peterson, D. L., and Westerling, A. L., 2009. Climate and wildfire area burned in western U. S. ecoprovinces, 1916-2003. Ecological Applications 19, 1003-1021.

McCoy, V. M., and Burn, C. R., 2005. Potential alteration by climate change of the forest-fire regime in the Boreal forest of central Yukon Territory. Arctic 58, 276-285.

Moritz, M. A., Parisien, M.-A., Batllori, E., Krawchuk, M. A., Dorn, J. V., Ganz, D. J., and Hayhoe, K., 2012. Climate change and disruptions to global fire activity. Ecosphere 3, doi:10.1890/ES11-00345.1.

National Wildfire Coordinating Group, 2005. National Fire Danger Rating System Weather Station Standards, 30 pp. (Available online: http://gacc.nifc.gov/oscc/administrative/policy_reports/myfiles/NFDRS_final_revmay05.pdf)

Pechony, O., and Shindell, D. T., 2009. Fire parameterization on a global scale. Journal of Geophysical Research 114, D16115, doi:10.1029/2009jd011927.

Philippi, T. E., 1993. Multiple regression: Herbivory, In: Scheiner, S., and Gurevitch, J. (Ed.), Design and Analysis of Ecological Experiments, Chapman & Hall, New York.

Prentice, I. C., Heimann, M., and Sitch, S., 2000. The carbon balance of the terrestrial biosphere: Ecosystem models and atmospheric observations. Ecological Applications 10, 1553-1573.

Price, C., and Rind, D., 1994. The Impact of a 2 x CO2 Climate on Lightning-Caused Fires. J. Clim. 7, 1484-1494.

Purves, D., and Pacala, S., 2008. Predictive models of forest dynamics. Science 320, 1452-1453, doi:10.1126/Science.1155359.

Rasilla, D. F., Garcia-Codron, J. C., Carracedo, V., and Diego, C., 2010. Circulation patterns, wildfire risk and wildfire occurrence at continental Spain. Physics and Chemistry of the Earth 35, 553-560, doi:10.1016/J.Pce.2009.09.003.

Rogers, B. M., Neilson, R. P., Drapek, R., Lenihan, J. M., Wells, J. R., Bachelet, D., and Law, B. E., 2011. Impacts of climate change on fire regimes and carbon stocks of the U.S. Pacific Northwest. Journal of Geophysical Research 116, doi:10.1029/2011jg001695.

Salathe, E. P., 2006. Influences of a shift in North Pacific storm tracks on western North American precipitation under global warming. Geophysical Research Letter 33, doi:10.1029/2006GL026882.

Schroeder, M., Glovinsky, M., Hendricks, V., Hood, F., Hull, M., Jacobson, H., Kirkpatrick, R., Krueger, D., Mallory, L., Oertel, A., Reese, R., Sergius, L., and Syverson, C., 1964. Synoptic weather types associated with critical fire weather, Pacific Southwest Forest and Range Experiment Station, Berkeley, CA.

Sitch, S., Smith, B., Prentice, I. C., Arneth, A., Bondeau, A., Cramer, W., Kaplan, J. O., Levis, S., Lucht, W., Sykes, M. T., Thonicke, K., and Venevsky, S., 2003. Evaluation of ecosystem dynamics, plant geography and terrestrial carbon cycling in the LPJ dynamic global vegetation model. Global Change Biology 9, 161-185.

Spracklen, D. V., Mickley, L. J., Logan, J. A., Hudman, R. C., Yevich, R., Flannigan, M. D., and Westerling, A. L., 2009. Impacts of climate change from 2000 to 2050 on wildfire activity and carbonaceous aerosol concentrations in the western United States. Journal of Geophysical Research 114, D20301, doi:10.1029/2008jd010966.

Thonicke, K., Spessa, A., Prentice, I. C., Harrison, S. P., Dong, L., and Carmona-Moreno, C., 2010. The influence of vegetation, fire spread and fire behaviour on biomass burning and trace gas emissions: results from a process-based model. Biogeosciences 7, 1991-2011, doi:10.5194/Bg-7-1991-2010.

Tymstra, C., Flannigan, M. D., Armitage, O. B., and Logan, K., 2007. Impact of climate change on area burned in Alberta's boreal forest. International Journal of Wildland Fire 16, 153-160, doi:10.1071/Wf06084.

Van Wagner, C. E., 1987. The development and structure of the Canadian forest fire weather index system, Canadian Forest Service, Forest Technical Report 35, Ottawa, Canada.

Westerling, A. L., Turner, M. G., Smithwick, E. A. H., Romme, W. H., and Ryan, M. G., 2011. Continued warming could transform Greater Yellowstone fire regimes by mid-

21st century. Proceedings of the National Academy of Sciences 108, 13165-13170, doi:10.1073/Pnas.1110199108.

Wu, S., Mickley, L. J., Kaplan, J. O., and Jacob, D. J., 2012. Impacts of changes in land use and land cover on atmospheric chemistry and air quality over the 21st century. Atmospheric Chemistry and Physics 12, 1597-1609, doi:10.5194/acp-12-1597-2012.

Yin, J. H., 2005. A consistent poleward shift of the storm tracks in simulations of 21st century climate. Geophysical Research Letter 32, doi:10.1029/2005GL023684.

Zhang, C., Tian, H., Wang, Y., Zeng, T., and Liu, Y., 2010. Predicting response of fuel load to future changes in climate and atmospheric composition in the Southern United States. Forest Ecology and Management 260, 556-564, doi:10.1016/j.foreco.2010.05.012.

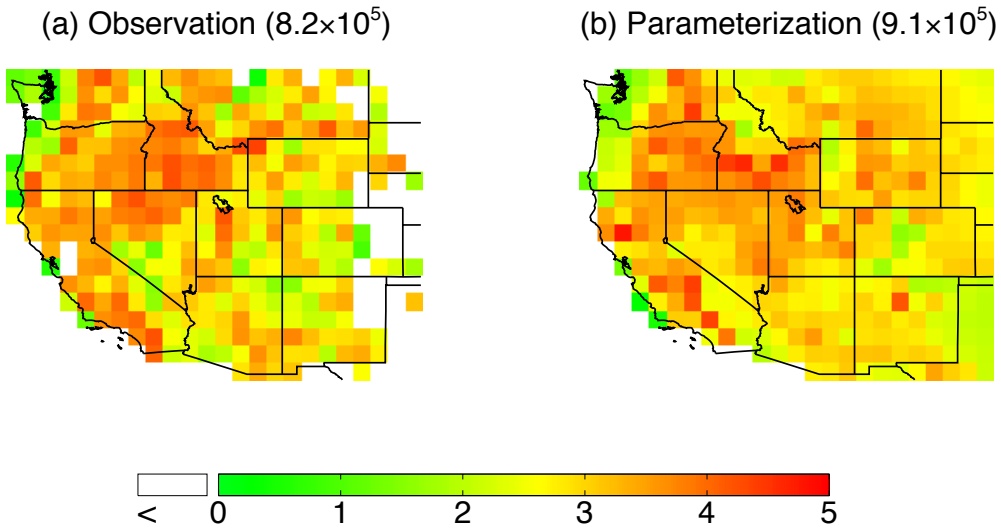

Fig. S1. Log10 of annual mean (a) observed and (b) simulated area burned (ha) averaged from 1980 to 2004. The simulated result is from the parameterization.

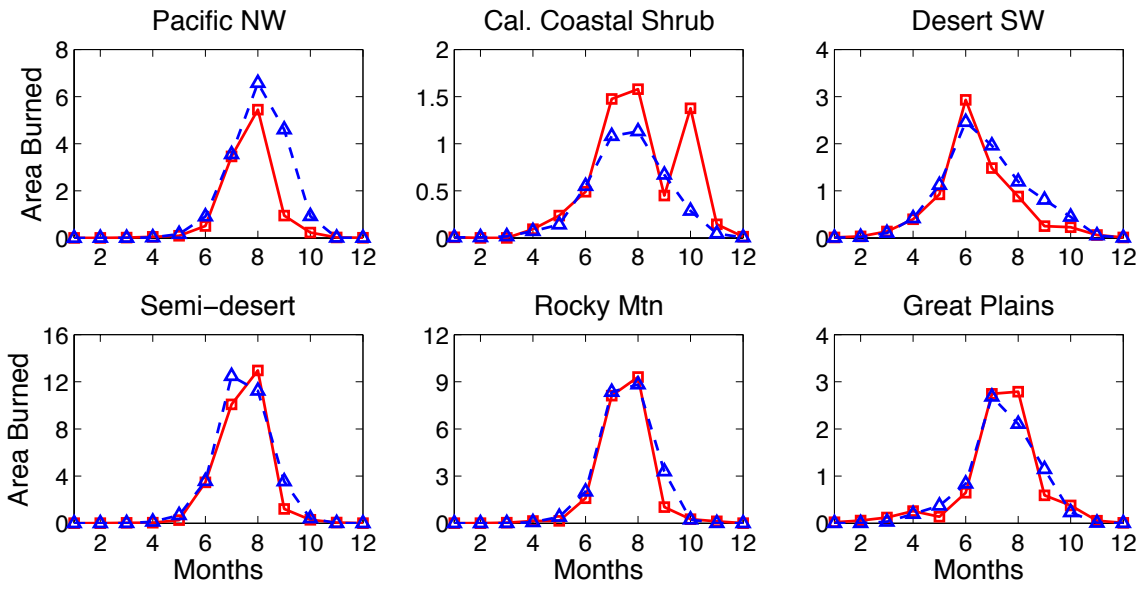

Fig. S2. Seasonality of simulated (blue dashed lines) and observed (red solid lines) area burned (10^4 ha) in each ecoregion. Simulations are from the parameterization. Each point represents the monthly mean for 1980-2004.

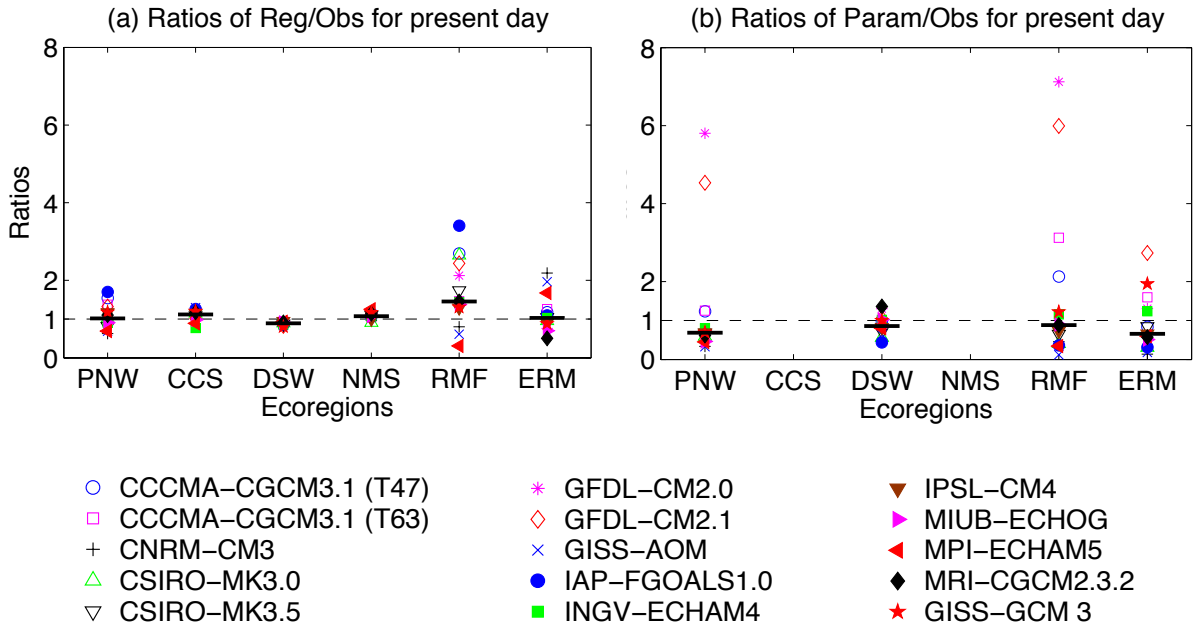

Fig. S3. (a) Ratios of predicted to observed present-day area burned. The simulated results are from the regressions. (b) Same as (a) but for results from the parameterization. The ecoregions are: PNW, Pacific Northwest; CCS, California Coastal Shrub; DSW, Desert Southwest; NMS, Nevada Mountains /Semi-desert; RMF, Rocky Mountains Forest; ERM, Eastern Rocky Mountains /Great Plains. Different symbols are used for each model. The short bold lines are the median ratios. No results are shown for the California Coastal Shrub and Nevada Mountains /Semi-desert regions in (b) because the parameterization does not reproduce the interannual variations of area burned there.

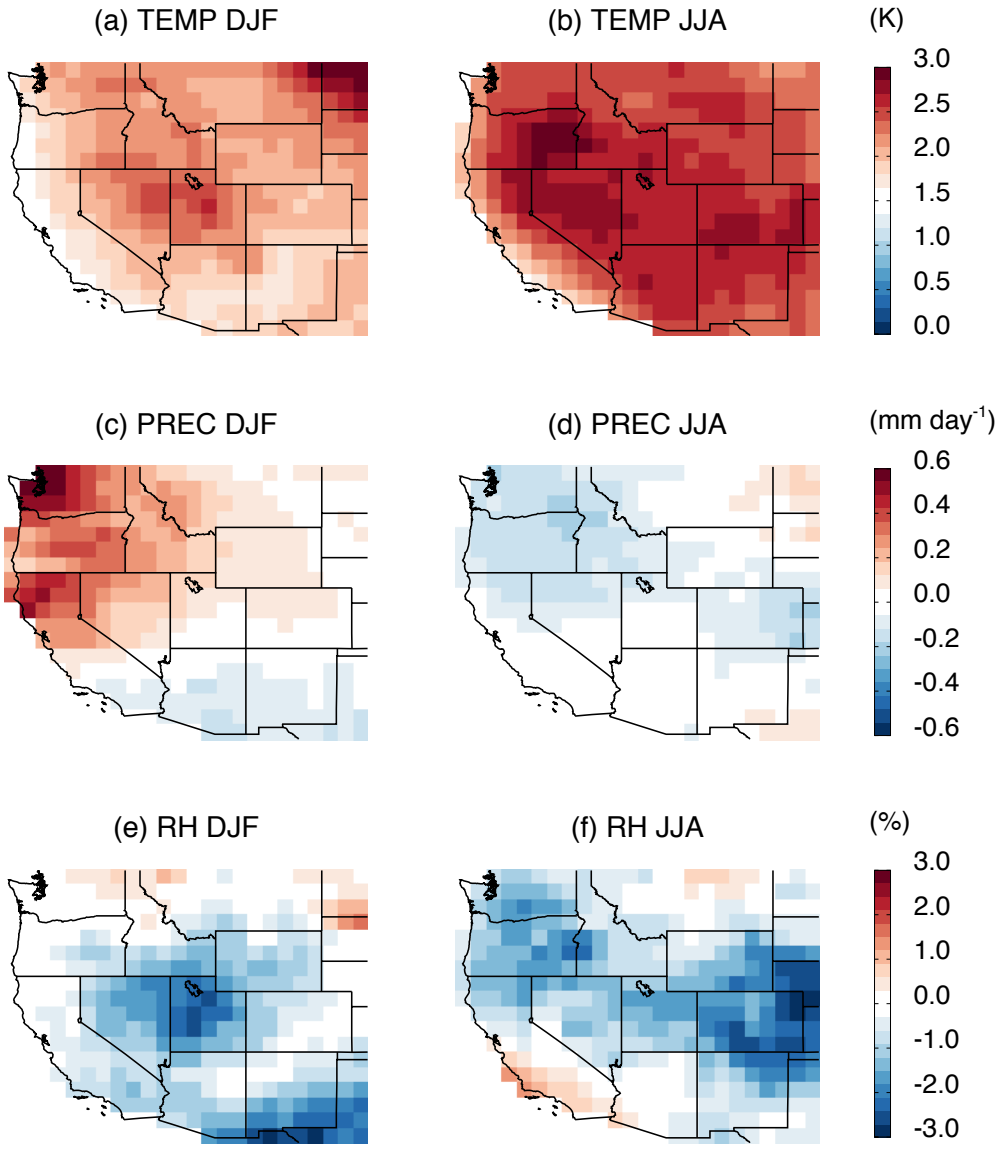

Fig. S4. Median changes in seasonal mean meteorological fields from 15 climate models following the A1B scenario for 2046-2065, relative to present-day (20C3M, 1981-2000) over western U.S. The left panels are for winter, the right panels for summer, with temperature, precipitation and relative humidity from top to bottom.

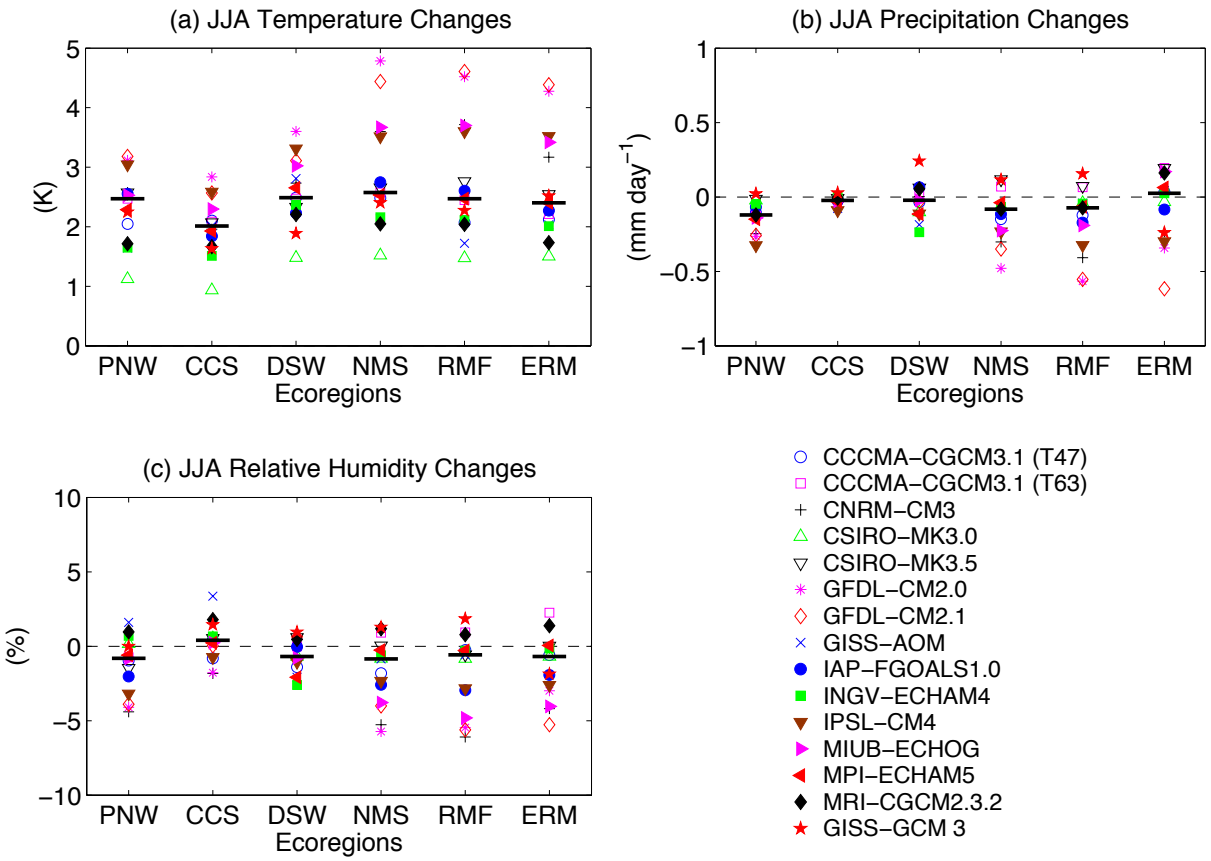

Fig. S5. Projected changes in (a) temperature, (b) precipitation, and (c) relative humidity for six ecoregions in summer by midcentury for 15 climate models. The ecoregions are: PNW, Pacific Northwest; CCS, California Coastal Shrub; DSW, Desert Southwest; NMS, Nevada Mountains /Semi-desert; RMF, Rocky Mountains Forest; ERM, Eastern Rocky Mountains /Great Plains. Different symbols are used for each model. The short bold lines are the median values.